

## Structure and Interactions of the Carboxyl Terminus of Striated Muscle $\alpha$ -Tropomyosin: It Is Important to be Flexible

Norma J. Greenfield, Thomas Palm, and Sarah E. Hitchcock-DeGregori

University of Medicine and Dentistry of New Jersey–Robert Wood Johnson Medical School, Piscataway, New Jersey 08854-5635 USA

**ABSTRACT** Tropomyosin (TM) binds to and regulates the actin filament. We used circular dichroism and heteronuclear NMR to investigate the secondary structure and interactions of the C terminus of striated muscle  $\alpha$ -TM, a major functional determinant, using a model peptide, TM9a<sub>251–284</sub>. The  $^1\text{H}^\alpha$  and  $^{13}\text{C}^\alpha$  chemical shift displacements show that residues 252 to 277 are  $\alpha$ -helical but residues 278 to 284 are nonhelical and mobile. The  $^1\text{H}^\text{N}$  and  $^{13}\text{C}'$  displacements suggest that residues 257 to 269 form a coiled coil. Formation of an “overlap” binary complex with a 33-residue N-terminal chimeric peptide containing residues 1 to 14 of  $\alpha$ -TM perturbs the  $^1\text{H}^\text{N}$  and  $^{15}\text{N}$  resonances of residues 274 to 284. Addition of a fragment of troponin T, TnT<sub>70–170</sub>, to the binary complex perturbs most of the  $^1\text{H}^\text{N}$ - $^{15}\text{N}$  cross-peaks. In addition, there are many new cross-peaks, showing that the binding is asymmetric. Q263, in a proposed troponin T binding site, shows two sets of side-chain  $^{15}\text{N}$ - $^1\text{H}$  cross-peaks, indicating conformational flexibility. The conformational equilibrium of the side chain changes upon formation of the binary and ternary complexes. Replacing Q263 with leucine greatly increases the stability of TM9a<sub>251–284</sub> and reduces its ability to form the binary and ternary complexes, showing that conformational flexibility is crucial for the binding functions of the C terminus.

### INTRODUCTION

The tropomyosins (TMs) are a highly conserved family of actin binding proteins found in most eukaryotic cells. They are two-chained parallel coiled-coil  $\alpha$ -helical proteins that bind cooperatively in the long pitch grooves of the helical actin filaments. Tropomyosin is critical for actin filament stabilization and for cooperative regulation of many actin functions (for review, see Gordon et al., 2000; Perry, 2001; Hitchcock-DeGregori, 2002).

The N- and C-terminal ends of the TMs play major roles in modulating actin affinity and in the cooperative regulation of contractile function with troponin (Tn) and myosin. The effects of removal of the ends are consistent with the proposal that the last 9 to 11 residues of TM interact with the first 9 to 11 residues of the N terminus to form an “overlap” complex, originally proposed by McLachlan and Stewart (McLachlan and Stewart, 1975; Tawada et al., 1975; Mak and Smillie, 1981; Dabrowska et al., 1983; Cho et al., 1990). In addition to their importance for N-terminal to C-terminal TM association and actin affinity, the presence of the C-terminal 9 to 11 amino acids is critical for the cooperative allosteric effects of myosin on thin filament activation by TM (Walsh et al., 1985; Heeley et al., 1989; Pan et al., 1989; Lehrer and Geeves, 1998; Moraczewska and Hitchcock-DeGregori, 2000).

The differences between smooth/nonmuscle and striated  $\alpha$ -TM in actin affinity, myosin S1-induced binding, and Tn affinity are largely defined by the C-terminal residues, in particular the C-terminal nine residues (Hammell and Hitch-

cock-DeGregori, 1996, 1997; Moraczewska and Hitchcock-DeGregori, 1998, 2000; Moraczewska et al., 1999). The entire region encoded by striated muscle specific exon 9a (residues 258–274), however, is required for Tn to promote fully high affinity actin binding with the first 18 residues being critical for the interaction of Tn with TM in the presence of  $\text{Ca}^{2+}$  (Hammell and Hitchcock-DeGregori, 1996). We have proposed that this region of TM forms a three-chained coiled coil with residues 92 to 110 of human cardiac TnT (Palm et al., 2001).

Circular dichroism and calorimetric studies have shown that the unfolding of TM as a function of temperature is not completely cooperative and that some regions of the TM molecule are more stable than others (Lehrer, 1975, 1978; Krishnan et al., 1978; Potekhin and Privalov, 1982; Privalov, 1982; Holtzer and Holtzer, 1990; Sturtevant et al., 1991; Ishii et al., 1992; Holtzer et al., 1995; Lehrer et al., 1997). It has been suggested that the flexibility of TM is essential for its end-to-end interactions and regulatory functions (Ohyashiki et al., 1976; Phillips et al., 1980; Phillips, 1986; Phillips and Chacko, 1996; Lehrer et al., 1997). Phillips et al. (1980), from examination of the motions of TM within crystals, suggested that the C-terminal half is very flexible and partially unfolded at physiological temperatures. Evidence that the C-terminal 9 to 11 “overlap” residues are highly flexible and different in structure from the bulk of the TM structure comes from a  $^1\text{H}$  NMR study in which several sharp peaks (indicative of regions of high flexibility) were lost upon carboxypeptidase removal of the last 9 to 11 residues (Stewart and Roberts, 1983).

Whereas the  $\alpha$ -helical coiled-coil structures of the N-termini of three TM variants are known at atomic level resolution (Greenfield et al., 1998, 2001; Brown et al., 2001), the structures of the C terminus and the overlap complex are not known. In the present work we used

Submitted May 10, 2002, and accepted for publication June 28, 2002.

Address reprint requests to Norma J. Greenfield, UMDNJ–Robert Wood Johnson Medical School, 675 Hoes Lane, Piscataway, NJ 08854-5635; Tel.: 732-235-5791; Fax: 732-235-4029; E-mail: greenfie@rwja.umdj.edu

© 2002 by the Biophysical Society

0006-3495/02/11/2754/13 \$2.00

**TABLE 1** Oligonucleotide, vector, and peptide DNA sequences

Oligonucleotide	Sequence
Oligo 1	CAGGAAACAGACCATATGTCGTAACC
Oligo 2	GATGAGAGAAGATCTGTGACCGTGATAC
His-tagged multicloning site from pProEX-HTb	CATATGTCGTAACCATCACCATCACCATACGATTACGATATCCCAACGACCGAA AACCTGTATTTTCAGGGCGCCATGGGATCCGGAATCAAAGGCCTACGTCGACGA GCTCAACTAGTGGCGCCGCTTTTCAATCTAGAGCCTGCAGTCTCGAGGCATGCGG TACCAAGCTTGGCTGTTTGGCGGATGAGAGAAGATCT
His-tagged TM9 <sub>251–284</sub> between NdeI and KpnI (coding sequence in italics)	CATATGTCGTAACCATCACCATCACCATCACCATACGATTACGATATCCCAACGACCGAAACC <i>CTGTATTTTCAGGGCTGCGGCAAAAGCATTGACGACTGGAAGACGAACCTTACGCTCAG</i> <i>AAACTTAAATACAAAGCTATCTCTGAAGAAGCTTGACCATGCTCTTAAAGACATGACTTCTA</i> <i>TCTAATAGAATTCAAAGGCCTACGTCGACGAGCTCAACTAGTGCAGGCGCTTTCG</i> <i>AATCTAGAGCCTGCAGTCTCGAGGCATGCGGTACC</i>
Oligo 3	GAGACGAACCTTTACGCGTTGAACTTAAATACAAAGCTATC
Oligo 4	GAAGACGAACCTTTACGCTGCGAAGCTTAAATACAAAGCTATC
Oligo 5	ATGGATGCGATCAAAAAAAAAATGCAGATGCTTAAGCTGGATAACTACCATCTTGA AAACGAAGTTGCTCGG
Oligo 6	GCCCTGAAAATACAGGTTTTCGGTC

three-dimensional NMR to determine the residue-specific secondary structure of the C-terminal region of striated  $\alpha$ -TM in a peptide. Our results show that the C-terminal seven residues of striated muscle  $\alpha$ -TM are not helical and are relatively mobile in solution. Upon complex formation with an N-terminal model TM peptide, the C-terminal 11 residues were perturbed. Formation of a ternary complex with a TnT peptide resulted in structural changes along the length of the C-terminal TM peptide. Of particular interest was that the mobile conformation of the side chain of Q263, postulated to be in a TnT binding site (Hammell and Hitchcock-DeGregori, 1996; Oliveira et al., 2000; Palm et al., 2001), changed upon complex formation. Evidence is provided to support the importance of the flexibility of this region of TM for functional interactions.

## MATERIALS AND METHODS

### Gene synthesis, peptide expression, and purification

The peptides used in this study were designed, expressed, and purified using methods similar to those previously reported (Greenfield et al., 2001). Briefly, DNA sequences were designed using DNA\* (DNASTAR, Inc., Madison, WI) to encode the desired amino acid sequence plus an N-terminal His-tag to facilitate purification. All the DNA sequences were confirmed by restriction analysis and automated sequencing (UMDNJ DNA Core Facility, Piscataway, NJ). Specific details of the gene designs are given below. The DNA was expressed in *Escherichia coli* using modified pET (Studier et al., 1990) and pSBET (Schenk et al., 1995) vectors. The cells were grown in minimal medium with either  $^{12}\text{C}$ - or  $^{13}\text{C}$ -uniformly labeled glucose and either  $^{14}\text{N}$ - or  $^{15}\text{N}$ -( $\text{NH}_4$ ) $_2\text{SO}_4$  as the sole sources of carbon and nitrogen. The His-tagged peptides were purified by affinity chromatography on Ni-NTA agarose column (Quiagen, Valencia, CA). Following isolation, the His-tags were removed with Tobacco Etch Virus protease, leaving an N-terminal glycine, and the peptides were purified to homogeneity using high-performance liquid chromatography.

### pET3-HTb, pET11-HTb, and pSBET-HTb vectors

Using polymerase chain reaction site-directed mutagenesis and the oligonucleotides 1 and 2 (Table 1) and their reverse complements, an *NdeI*-site and a *BglII*-site were created in pProEX HTb (Life Technologies, Rockville, MD) before the sequence for the His-tag and after the multicloning site, respectively (Table 1). The DNA was digested with *NdeI* and *BglII*, and the fragment with the multicloning site and the His-tag was cloned into pSBETc, pET3a, and pET11a cut with *NdeI* and *BamHI*.

### TM9<sub>251–284</sub>

The DNA encoding His-tagged TM9<sub>251–284</sub> was cloned into pSBET-HTb between *NdeI* and *KpnI* and expressed in *E. coli* BL21(DE3) pLysS (Table 1). The purified peptide was cross-linked by air oxidation of the cysteine residues at pH 8.0 to form a disulfide as previously described (Palm et al., 2001).

### Q263L-TM9<sub>251–284</sub> and Q263A-TM9<sub>251–284</sub>

Q263 of TM9<sub>251–284</sub> was changed to leucine by polymerase chain reaction site-directed mutagenesis using the oligonucleotides 3 (Table 1) and its reverse complement. These oligonucleotides were designed to contain an analytical *MluI*-site to facilitate the selection of positive clones. In the same manner, Q263 was changed to alanine using the oligonucleotides 4 (Table 1) and its reverse complement. These oligonucleotides introduce an analytical *HindIII*-site. The Q263L-TM9<sub>251–284</sub> DNA was cloned into pET11-HTb between *NdeI* and *KpnI* and expressed in *E. coli* BL21(DE3). The Q263A-TM9<sub>251–284</sub> DNA was cloned into pET3-HTb between *NdeI* and *KpnI* and expressed in *E. coli* BL21(DE3) pLysS. Both peptides were isolated, cross-linked, and purified in the same manner as the wild-type peptide.

### TM1a<sub>1–14</sub>

TM1a<sub>1–14</sub> has the sequence of TMZip (Greenfield et al., 1998) (also called AcTM1aZip (Greenfield and Fowler, 2002)) previously described with an N-terminal glycine residue replacing the N-terminal acetyl moiety in TMZip. The synthetic gene for His-tagged TM1a<sub>1–14</sub> was generated from SfoI-digested GlyTM1bZip in pProEX HTa (Greenfield et al., 2001) using the oligonucleotides 5 and 6 (Table 1). An *NdeI* site was introduced at the

5'-end of the initiating ATG using oligo 1 and its reverse complement to allow cloning into pET3-HTb between *Nde*I and *Kpn*I. TM1a<sub>1-14</sub> was expressed in *E. coli* BL21(DE3) pLysS. Acetylated TM1a<sub>1-14</sub> (AcTM1a<sub>1-14</sub>, originally referred to as TMZip and AcTM1aZip (Greenfield et al., 1998; Greenfield and Fowler, 2002)) was purchased from SynPep Corp. (Dublin, CA).

### TnT<sub>70-170</sub>

A fragment of human cardiac TnT, TnT<sub>70-170</sub>, was expressed and purified as previously described (Palm et al., 2001).

## Circular dichroism spectroscopy

Circular dichroism studies were performed as described previously (Palm et al., 2001). The dissociation constants of the TM9a<sub>251-284</sub>/AcTM1a<sub>1-14</sub> complexes were estimated from the differences in the ellipticity at 222 nm as a function of temperature of the individual peptides and complexes assuming that one molar equivalent of the complex cooperatively dissociates to yield one molar equivalent of unfolded TM9a<sub>251-284</sub> and two molar equivalents of unfolded AcTM1a<sub>1-14</sub>, as described previously (Greenfield and Fowler, 2002). The helical content of the TM9a<sub>251-284</sub> peptides were estimated from the ellipticity as a function of wavelength using the program CDNN (Böhm et al., 1992).

## Native gel electrophoresis

Samples for electrophoresis were all prepared in 10 mM potassium phosphate, pH 6.5, containing 10% glycerol. Native gel electrophoresis was carried out as described by Katayama and Nozaki (1982) with the following modifications: 10% acrylamide/bis-acrylamide (30:0.8) glycerol slabs (10 cm × 6 cm) were prepared in 20 mM Tris-HCl and 120 mM glycine, pH 8.8, containing 10% glycerol. Samples were separated at constant voltage (150 V) until a bromophenol blue marker was at the end of the gel (1.5 h).

## NMR measurements

NMR data were collected on a Varian Inova 600 spectrometer (Varian, Inc., Palo Alto, CA) equipped with four independent channels. All spectral measurements were made in susceptibility-matched NMR tubes (Shigemi, Inc., Allison Park, PA) at 10°C. All samples were dissolved in 100 mM NaCl, 10 mM sodium phosphate, pH 6.4. The program VNMR (Varian, Inc.) was used for data processing. The program Sparky (T. Goddard and T. Kneller, University of California at San Francisco, unpublished data) was used for peak peaking (i.e., finding the centers of the cross-peaks) and manual alignment of the spectra.

## Backbone resonance assignments

The assignments of the resonances of the N, H, C<sup>α</sup>, C<sup>β</sup>, C', and H<sup>α</sup> atoms were determined as described previously (Greenfield et al., 2001), but the resonances were aligned manually rather than automatically since some of the spectra were unsuitable for use with the program AutoAssign (Zimmerman et al., 1997) due to poor transfer of magnetization.

## RESULTS

### Peptide design

We have developed a model system to study the structures of the ends of TM and complex formation with the TM

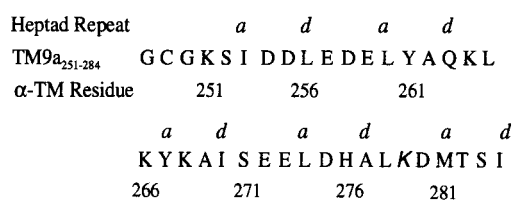


FIGURE 1 Sequence of TM9a<sub>251-284</sub>. The last 34 residues correspond to the sequence of the C terminus of full-length striated α-tropomyosin and are numbered according to the sequence of the full length protein. In addition, the peptide has a three amino acid extension at its N terminus, GCG. In TM9a<sub>251-284</sub>, N279 of wild-type α-TM is replaced with lysine, as shown in italics. Residues at the *a* and *d* position of the coiled-coil heptad repeat are labeled.

binding domain of TnT in solution (Palm et al., 2001). The model was originally used to investigate the effect of disease-causing mutations in TnT on binding to TM where the TM peptides were chemically synthesized. Here the TM peptides have been modified to allow the production of recombinant peptides in *E. coli* for structural studies.

### C-terminal tropomyosin peptide, TM9a<sub>251-284</sub>

A 37-residue peptide, TM9a<sub>251-284</sub>, based on a peptide used in previous studies (Palm et al., 2001), was designed to study the structure and binding functions of the C terminus of striated muscle α-TM (Fig. 1). TM9a<sub>251-284</sub> contains the last 34 C-terminal residues of striated muscle α-TM: residues 251 to 257 encoded by exon 8 followed by residues 258 to 284 encoded by the striated muscle-specific exon 9a of the rat α-TM gene (Ruiz-Opazo and Nadal-Ginard, 1987). Three residues, GCG, precede the TM sequence. The cysteine was placed at the first N-terminal *d* position of the coiled-coil heptad repeat to allow oxidative cross-linking of the peptide via disulfide formation, which stabilizes coiled-coils (Lehrer, 1975; Hodges et al., 1981; Zhou et al., 1993; Greenfield et al., 1994). The initial glycine is left following Tobacco Etch Virus protease cleavage of the His tag, and a glycine following the cysteine was included to relieve strain caused by disulfide formation.

TM9a<sub>251-284</sub> was designed using the rat striated α-TM sequence from the Protein Information Resource protein data bank, locus B27407. The data base sequence contains an error with a lysine instead of asparagine at residue 279, as was correctly published (Ruiz-Opazo and Nadal-Ginard, 1987). The mutation N279K did not change the peptide's binding properties for the TM N terminus or a TnT fragment (Palm et al., 2001) but advantageously increased the T<sub>M</sub> of unfolding of TM9a<sub>251-284</sub> from 16°C to 24°C, allowing the present NMR structural studies at 10°C.

### Design of the N-terminal tropomyosin peptide, TM1a<sub>1-14</sub>

The N-terminal peptide contains the first 14 N-terminal residues found in long rat α-TM isoforms, including striated

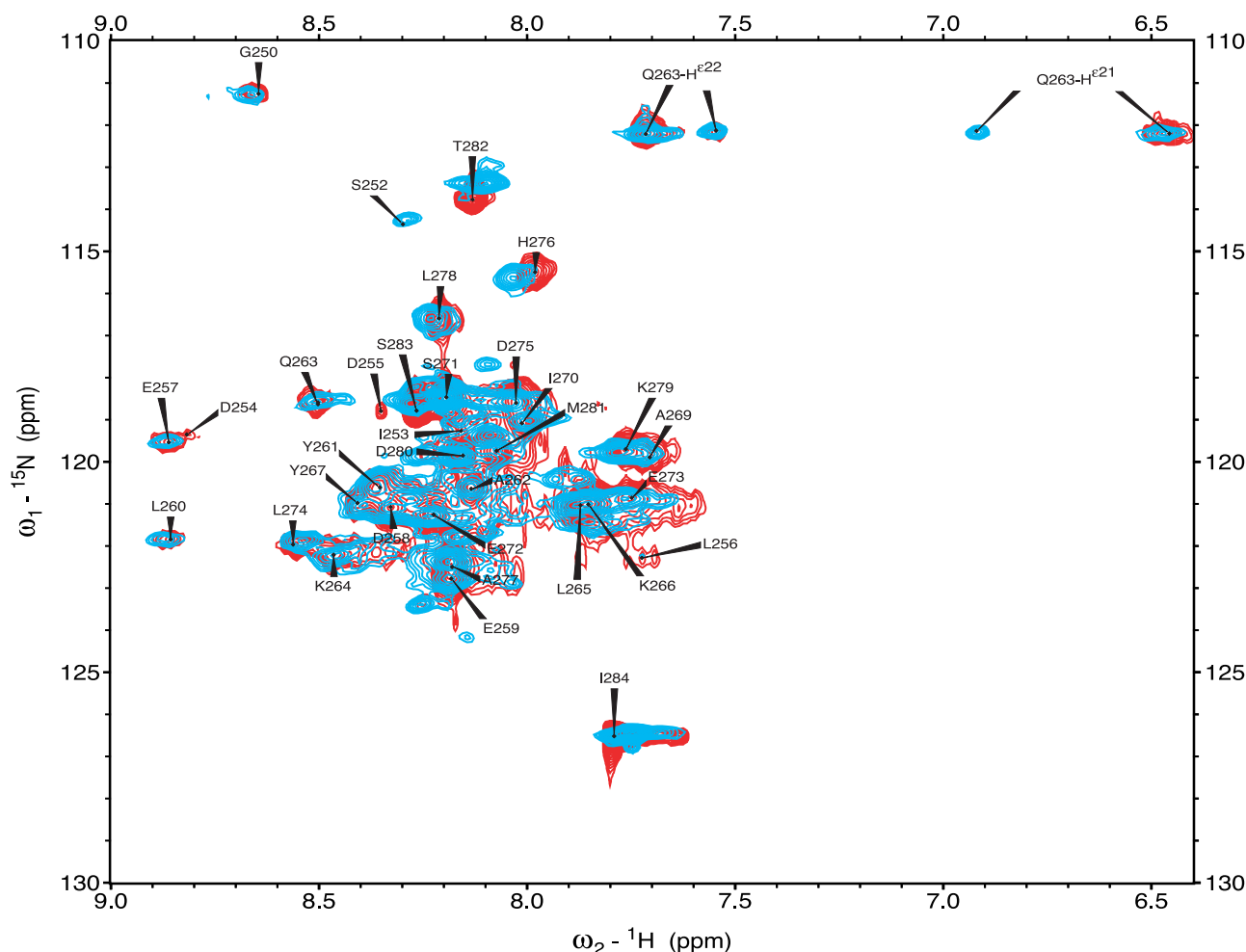


FIGURE 2 The  $^1\text{H}$ - $^{15}\text{N}$ -HSQC spectra of  $^{15}\text{N}$ -TM9a<sub>251–284</sub> alone, 0.4 mM, (red) and its complex, 0.2 mM, with unlabeled TM1a<sub>1–14</sub> (cyan). The cross-peaks are labeled with the residue number corresponding to full-length rat striated-muscle  $\alpha$ -TM. The Q263 side chain exhibits two sets of amide cross-peaks. Formation of a 1:1 complex with unlabeled TM1a<sub>1–14</sub> results in displacements of the cross-peaks arising from the most of the backbone amides of residues 274 to 284 and causes a large change in the relative intensities of the two sets cross-peaks arising from the Q263 side chain.

muscle TM, and the last 18 C-terminal residues of the GCN4 (a yeast transcriptional activator of amino acid biosynthetic genes) yeast transcription factor leucine zipper (Landschulz et al., 1988). In TM1a<sub>1–14</sub>, M1 is preceded by a glycine residue, which remains following cleavage of the His-tag from the *E. coli* expressed peptide (see Materials and Methods). We previously determined the structure of the chemically synthesized peptide in which the initial methionine was N-acetylated (TMZip (Greenfield et al., 1998), also called AcTM1aZip (Greenfield and Fowler, 2002)). Replacing the acetyl group with glycine lowered the stability of the peptide from 28°C to 21°C at a concentration of 15  $\mu\text{M}$  but did not change the ellipticity when folded. At 1 mM, the concentration used for the NMR studies, TM1a<sub>1–14</sub> has a fully folded two-chain coiled-coil conformation. TM1a<sub>1–14</sub> formed binary complexes with TM9a<sub>251–284</sub> and ternary complexes with the C-terminal peptide and TnT<sub>70–170</sub> with almost the same affinity as the acetylated peptide

(Palm, T., N. J. Greenfield, and S. E. Hitchcock-Degregori, manuscript in preparation). It also had the same binding affinity as the acetylated peptide for tropomodulin (Greenfield and Fowler, 2002).

## Secondary structure determination of TM9a<sub>251–284</sub>

### Sequential assignments

The  $^1\text{H}$ - $^{15}\text{N}$  heteronuclear single quantum coherence (HSQC) spectrum of TM9a<sub>251–284</sub> (Fig. 2) resolved 30 of the expected 36 backbone peaks, and two intense peaks attributed to the side chain of Q263. At a lower intensity threshold four additional backbone  $^1\text{H}$  resonances were observed as well as a minor set of Q263 side-chain cross-peaks. Most of the backbone atoms of TM9a<sub>251–284</sub> were uniquely assigned using NMR techniques that detect signals arising from atoms linked to each other through covalent



**TABLE 2** Experimental details of spectra used to assign the resonances of TM9a<sub>251–284</sub>

Spectrum	Label	Concen- trations mM	$\omega$ 1 atoms	Nuclei			Data size			Assign- ments	References
				$\omega$ 1	$\omega$ 2	$\omega$ 3	$\omega$ 1	$\omega$ 2	$\omega$ 3		
Backbone											
$^{15}\text{N}$ - $^1\text{H}$ HSQC	$^{15}\text{N}$	0.4	N	$^{15}\text{N}$	$^1\text{H}$		512	1024		36	(Bodenhausen and Ruben, 1980; Kay et al., 1992)
HN(CA)CO	$^{15}\text{N}$ , $^{13}\text{C}$	0.4	Carbonyl	$^{13}\text{C}$	$^{15}\text{N}$	$^1\text{H}$	256	128	256	9	(Clubb et al., 1992)
HNCO	$^{15}\text{N}$ , $^{13}\text{C}$	0.4	Carbonyl	$^{13}\text{C}$	$^{15}\text{N}$	$^1\text{H}$	256	128	256	32	(Boucher et al., 1991; Feng et al., 1996)
H(CA)(CO)NH	$^{15}\text{N}$ , $^{13}\text{C}$	1.4	H $^{\alpha}$	$^1\text{H}$	$^{15}\text{N}$	$^1\text{H}$	256	128	256	27	(Muhandiram and Kay, 1994)
H(CA)NH	$^{15}\text{N}$ , $^{13}\text{C}$	1.4	H $^{\alpha}$	$^1\text{H}$	$^{15}\text{N}$	$^1\text{H}$	256	128	256	50	(Montelione and Wagner, 1989, 1990; Feng et al., 1996)
CA(CO)NH	$^{15}\text{N}$ , $^{13}\text{C}$	1.4	C $^{\alpha}$	$^{13}\text{C}$	$^{15}\text{N}$	$^1\text{H}$	256	128	256	26	(Boucher et al., 1991; Feng et al., 1996)
CANH	$^{15}\text{N}$ , $^{13}\text{C}$	0.4	C $^{\alpha}$	$^{13}\text{C}$	$^{15}\text{N}$	$^1\text{H}$	256	128	256	62	(Montelione and Wagner, 1989, 1990; Feng et al., 1996)
CBCA(CO)NH	$^{15}\text{N}$ , $^{13}\text{C}$	1.4	C $^{\alpha}$ and C $^{\beta}$	$^{13}\text{C}$	$^{15}\text{N}$		512	1024	256	12	(Grzesiek and Bax, 1992a,b; Rios et al., 1996)
CBCANH	$^{15}\text{N}$ , $^{13}\text{C}$	1.4	C $^{\alpha}$ and C $^{\beta}$	$^{13}\text{C}$	$^{15}\text{N}$	$^1\text{H}$	256	128	256	47	(Grzesiek and Bax, 1992a,b; Rios et al., 1996)
Side Chain											
HCCH-cosy	$^{15}\text{N}$ , $^{13}\text{C}$	1.4	H	$^1\text{H}$	$^{13}\text{C}$	$^1\text{H}$	256	128	256	199	(Bax et al., 1990; Kay et al., 1990)
CCH-cosy	$^{15}\text{N}$ , $^{13}\text{C}$	1.4	C	$^{13}\text{C}$	$^{13}\text{C}$	$^1\text{H}$	256	128	256	200	(Bax et al., 1990; Kay et al., 1990)
$^{13}\text{C}$ - $^1\text{H}$ -HSQC	$^{15}\text{N}$ , $^{13}\text{C}$	0.4	C		$^{13}\text{C}$	$^1\text{H}$		256	1024	64	(Bodenhausen and Ruben, 1980)

bonds. To assign the <sup>13</sup>C, <sup>15</sup>N, and <sup>1</sup>H resonances of the backbone atoms, eight heteronuclear three-dimensional-NMR spectra were collected. The details of the parameters used for data collection of these spectra are summarized in Table 2. Four of the spectra (HNCO, CA(CO)NH, CBCA(CO)NH, and H(CA)(CO)NH) exhibited cross-peaks between the <sup>13</sup>C atoms or protons of a given residue (*i*) to the <sup>15</sup>N and <sup>1</sup>H atoms of the sequential residue (*i* + 1). The other four spectra (HNCACO, CANH, CBCANH, and H(CA)NH) showed cross-peaks to the <sup>15</sup>N and <sup>1</sup>H atoms of both the same residue (*i*) as well as the sequential (*i* + 1) residue. By aligning the CANH and CA(CO)NH spectra and the H(CA)NH and H(CA)(CO)NH peaks it was possible to assign uniquely and sequentially most of the cross-peaks observed in the <sup>1</sup>H-<sup>15</sup>N HSQC spectrum. These “through-bond” connections are summarized in Fig. 3. The CA(CO)NH, CBCANH, and CBCA(CO)NH had very low signal-to-noise and could only be used to confirm the assignments of the last nine residues. Two residues, Lys-251 and Glu-272, had identical <sup>1</sup>H-<sup>15</sup>N cross-peaks but could be assigned on the basis of their unique C $^{\alpha}$  reso-

nances. The <sup>1</sup>H $^{\alpha}$ , <sup>1</sup>H<sup>N</sup>, and <sup>13</sup>C $^{\alpha}$  resonances of Asp-255 and Asp-256 were very broad in the “through bond” data sets, but their assignments were confirmed using <sup>13</sup>C- and <sup>15</sup>N-edited nuclear Overhauser effect spectroscopy data (unpublished results).

#### Secondary structure of TM9a<sub>251–284</sub>

The chemical shifts of <sup>1</sup>H $^{\alpha}$ , <sup>1</sup>H<sup>N</sup>, <sup>13</sup>C, and <sup>13</sup>C $^{\alpha}$  atoms (Fig. 4) provided information about the secondary structure and coiled-coil domain of TM9a<sub>251–284</sub>. At 10°C the displacements of the chemical shifts compared with reference values and periodicity of the displacements, showed that residues 252 to 277 are  $\alpha$ -helical and that residues 257 to 269 appear to form a coiled coil. The <sup>1</sup>H $^{\alpha}$  and <sup>13</sup>C $^{\alpha}$  resonances of the last four residues were not displaced, showing that they are not helical. In addition, the cross-peaks from these residues in the HNCO, CANH, CA(CO)NH, H(CA)NH, and H(CA)(CO)NH spectra had very high relative intensities, suggesting that they are mobile.

The H<sup>N</sup> resonances of coiled coils display a characteristic periodicity (Oas et al., 1990; Goodman and Kim, 1991; Junius et al., 1996; Marti et al., 2000). Such periodicity was seen for residues 257–269, suggesting that they form a coiled coil, but no clear periodicity was seen for residues 270–280, suggesting that, although they are helical, they do not form a coiled coil. Note that Li et al. (2002) have recently published an x-ray structure of a C-terminal chimeric peptide containing residues 253–284 of striated  $\alpha$ -TM, which shows that residues 263–280 are helical but do not form a coiled coil. Their structure, however, cannot be directly compared to TM9a<sub>251–284</sub>, because the chimeric peptide was crystallized at pH 8.3 under conditions where it formed a C-terminal to C-terminal binary complex. No such complex formation is seen for TM9a<sub>251–284</sub>, which was studied at pH 6.5 at physiological ionic strength.

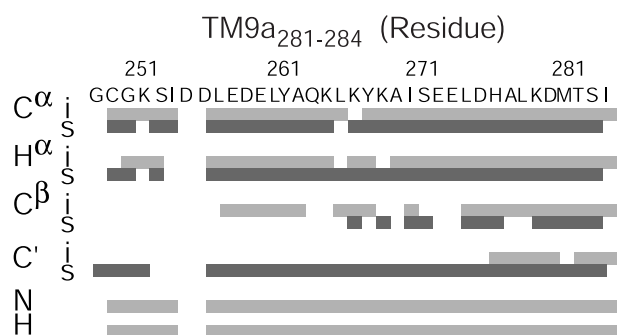


**FIGURE 3** Summary of the intra residue (light gray) and sequential (dark gray) connectivity data used to determine the sequential assignments of TM9a<sub>251–284</sub>.

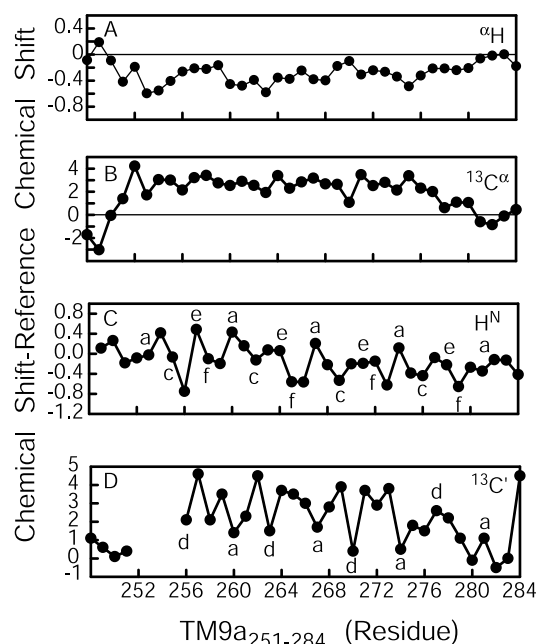


FIGURE 4 Displacements of the chemical shifts of TM9a<sub>251-284</sub> compared with those of statistical coils. The chemical shifts of the  $^1\text{H}^\alpha$  protons of residues 252 to 277 (A) were displaced upfield, whereas the  $^{13}\text{C}^\alpha$  resonances (B) were displaced downfield, consistent with these residues being in an  $\alpha$ -helical conformation (Wishart et al., 1992; Wishart and Sykes, 1994). The displacements of the  $\text{H}^\text{N}$  protons (C) of residues 257 to 269 had the periodicity characteristic of coiled-coil proteins in that the chemical shifts of the  $\text{H}^\text{N}$  protons in *a* and *e* positions of the coiled-coil heptad repeat were displaced downfield, whereas those of the *c* and *f* positions were displaced upfield relative to those of references for disordered peptides (Oas et al., 1990; Goodman and Kim, 1991; Junius et al., 1996; Marti et al., 2000). The  $^{13}\text{C}$  chemical shifts (D) of residues 256 to 274 also had properties seen in other coiled-coil peptides in that the resonances of *a* and *d* residues were displaced upfield relative to those of the adjacent residues (Greenfield et al., 2001). The  $^1\text{H}^\alpha$  and  $^{13}\text{C}^\alpha$  resonances of the last four residues were not displaced showing that they are not helical. The reference chemical shifts for  $\text{H}^\alpha$ ,  $\text{H}^\text{N}$ ,  $^{13}\text{C}'$ , and  $^{13}\text{C}^\alpha$  are from Wishart (Wishart et al., 1992; Wishart and Sykes, 1994).

### Effect of complex formation with an N-terminal tropomyosin peptide

Addition of a molar equivalent of unlabeled TM1a<sub>1-14</sub>, the chimeric peptide containing the first 14 N-terminal residues of striated  $\alpha$ -TM and the last 18 residues of GCN4, to TM9a<sub>251-284</sub> to form an “overlap” complex caused significant displacements of some of the cross-peaks in the  $^{15}\text{N}$ - $^1\text{H}$  HSQC spectrum of TM9a<sub>251-284</sub> (Fig. 2). The chemical shift displacements of the cross-peaks in the  $^{15}\text{N}$ - $^1\text{H}$  HSQC arising from the backbone upon complex formation were largest for residues 274 to 277 and 280 to 284, postulated to be in the TM overlap region (Fig. 5) (McLachlan and Stewart, 1975). The displacements of the  $\text{H}^\text{N}$  chemical shifts of these residues (Fig. 2) were relatively minor, however, suggesting that binary complex formation does not result in increased (or changed) coiled-coil content.

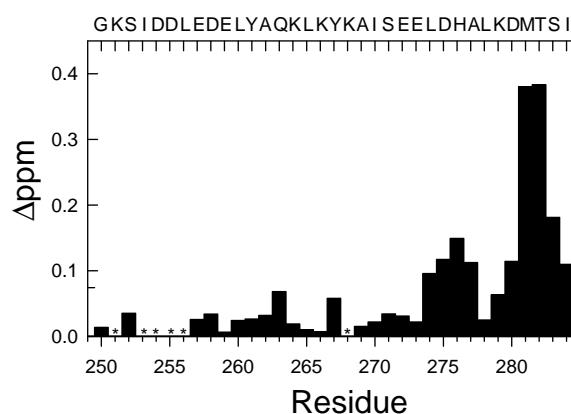


FIGURE 5 Chemical shift displacements,  $\Delta$  ppm, of the cross-peaks in the  $^{15}\text{N}$ - $^1\text{H}$  HSQC spectrum of TM9a<sub>251-284</sub> upon complex formation with TM1a<sub>1-14</sub>.  $\Delta$  ppm is defined as the square root of the sum of the squares of the displacements of the chemical shifts of the  $^1\text{H}$  and  $^{15}\text{N}$  resonances upon complex formation. The largest changes were seen in the  $^{15}\text{N}$  resonances of residues 274 to 284, postulated to form an overlap complex with the N terminus.

The most dramatic changes in the HSQC spectrum were in the cross-peaks arising from the side-chain of Q263. In TM9a<sub>251-284</sub> there were two sets of Q263 side-chain cross-peaks, a major set with proton chemical shifts at 7.55 and 6.47 and a minor set with proton chemical shifts of 7.71 and 6.91 ppm. These peaks were almost equal in intensity in the overlap complex with TM1a<sub>1-14</sub>. The minor set of cross-peaks in the unbound C-terminal peptide had chemical shifts very close to those found for unstructured short glutamine containing peptides (Schwarzinger et al., 2000), although they did not coincide with peaks observed when the temperature was raised, showing that they did not arise from unfolded peptide.

In addition to causing displacements of the backbone amide resonances, binding to TM1a<sub>1-14</sub> caused several of the backbone cross-peaks to split slightly into two overlapping peaks, suggesting that the structure of TM9a<sub>251-284</sub> in the complex is asymmetric. This effect was most pronounced for the cross-peaks arising from the overlap region (residues 274, 276, and 280 to 284), although cross-peaks arising from residues 262 to 264 also exhibited slight splitting. (Note that, at the concentration of the complex used for the HSQC spectrum, 0.2 mM, all of the 9a peptide was in the form of the complex, because the dissociation constant of the complex of TM1a<sub>1-14</sub> and TM9a<sub>251-284</sub> is  $\sim 2 \mu\text{M}$ ).

### Effect of ternary complex formation with the N-terminal TM peptide and a troponin T fragment

A human cardiac TnT fragment, TnT<sub>70-170</sub>, that contains the  $\text{Ca}^{2+}$  independent TM binding site, forms a stable ternary complex with the “overlap” complex of N- and C-terminal TM peptides (Palm et al., 2001). Formation of

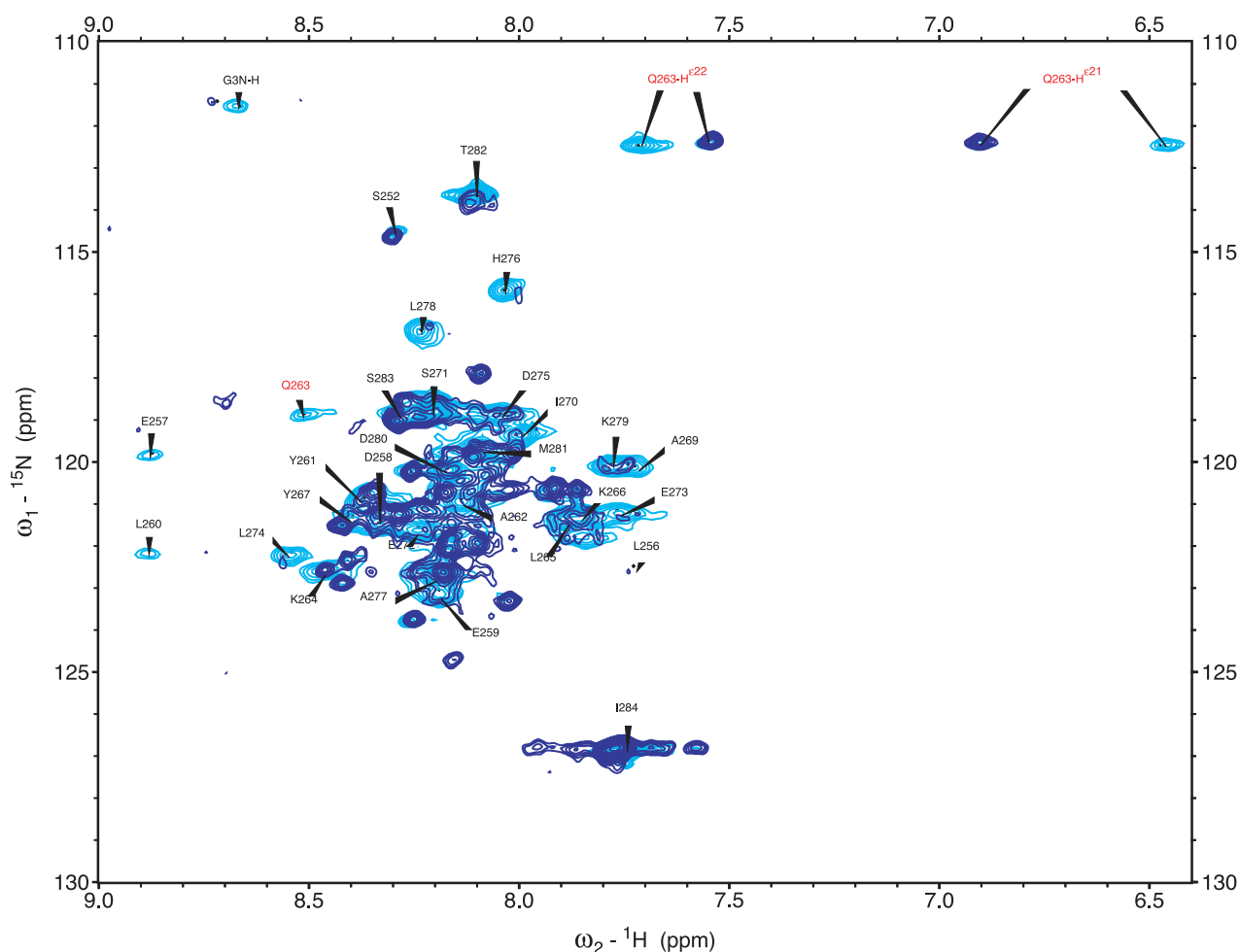


FIGURE 6  $^1\text{H}$ - $^{15}\text{N}$ -HSQC spectra of the complex, 0.2 mM, of  $^{15}\text{N}$ -TM9a<sub>251–284</sub> with unlabeled TM1a<sub>1–14</sub> (cyan) and the ternary complex, 0.1 mM, of  $^{15}\text{N}$ -TM9a<sub>251–284</sub> with unlabeled TM1a<sub>1–14</sub> and an unlabeled TnT fragment, TnT<sub>70–170</sub> (dark blue). Formation of a ternary complex of TM9a<sub>251–284</sub> with TM1a<sub>1–14</sub> and TnT<sub>70–170</sub> shifted or broadened most of the original cross-peaks arising from the uncomplexed C-terminal peptide and increased the total number of resolved, high-intensity peaks to 50.

the ternary complex caused changes in the entire HSQC spectrum (Fig. 6, binary complex, cyan; ternary complex, dark blue). Many of the cross-peaks were shifted or broadened and more than 10 additional cross-peaks appeared. A total of 50 cross-peaks were well resolved in the ternary complex, showing that the equivalent residues from the two peptide chains of TM9a<sub>251–284</sub> have different environments when TnT is bound to overlap complex. In the ternary complex, the original strong set of Q263 side-chain cross-peaks seen in the unbound TM9a<sub>251–284</sub> spectrum has disappeared and only the “minor” set is visible. In addition, the cross-peak arising from the Q263 backbone (numbered in red in Fig. 6) is either totally broadened or shifted. It is possible that the cross-peaks arising from the two Q263 residues in TM9a<sub>251–284</sub> (one from each chain) have identical chemical shifts when TnT<sub>70–170</sub> is bound. A more likely explanation, however, is that the Q263 side chain from one peptide chain is bound to the TnT peptide and its cross-peak is broadened (either by slow tumbling or ex-

change broadening) and the other side chain is more open to the solvent and is tumbling more rapidly giving a strong peak with a chemical shift close to those seen in disordered peptides. Recently, de Sousa and Farah (2001) found that when Q263 was replaced by a fluorescent probe, 5-hydroxytryptophan, the fluorescence was sensitive to the binding of Tn, consistent with Q263 being in the Tn binding site.

### The effects of mutations of Q263 on the structure and binding behavior of TM9a<sub>251–284</sub>

#### Circular dichroism studies

The dramatic change in the Q263 side chain upon complex formation suggested that its conformational flexibility may be important for the binding interactions of the C terminus of striated  $\alpha$ -TM. Q263 is at the coiled-coil interface in a *d* position where it would be expected to destabilize a two-chain coiled coil. To test the influence of coiled-coil stabil-

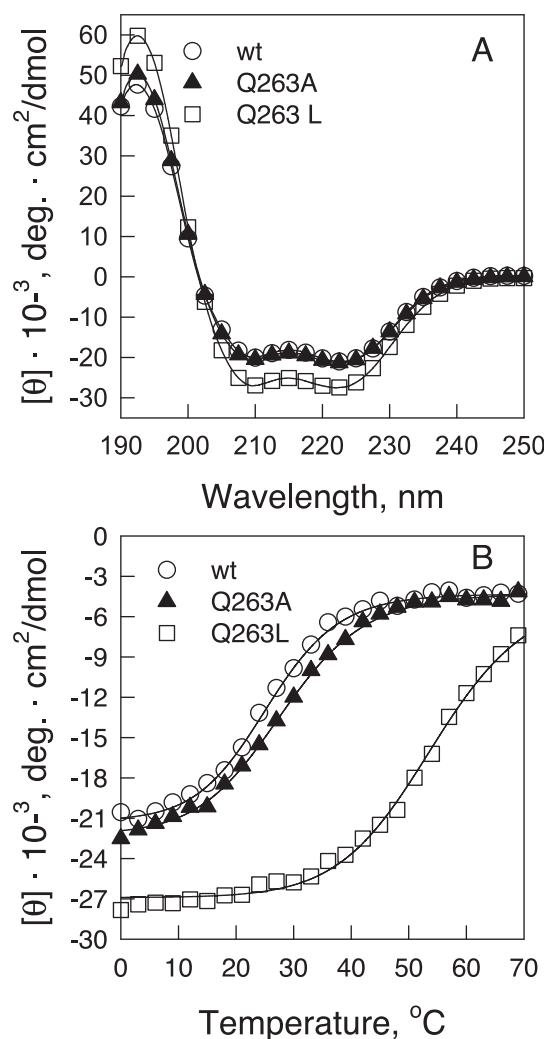


FIGURE 7 Effect of mutations of Q263 on the circular dichroism spectrum and stability of TM9<sub>a251-284</sub>. Changing the glutamine to alanine had little effect on structure or stability, but mutating it to leucine increased both the helical content and stability. (A) Circular dichroism spectra of (○) wt-, (□) Q263L-, and (▲) Q263A-TM9<sub>a251-284</sub>. (B) Ellipticity at 222 nm of TM9<sub>a251-284</sub> and its Q263L and Q263A mutants as a function of temperature. Symbols same as Fig. 6 A. All of the peptides were 10  $\mu$ M in potassium phosphate buffer, 10 mM, pH 6.5.

ity of this region on complex formation, we replaced Gln-263 with Ala, which should allow for similar coiled-coil stability and with Leu to strongly stabilize the coiled coil (Tripet et al., 2000). The Q263L mutation increased the helical content of the TM9<sub>a251-284</sub> at 0°C from 58% to 76% and the  $T_M$  of unfolding from 25°C to 57°C. In contrast, the Q263A mutation had only a slight effect on the helical content (58% to 61%, Fig. 7 A) and increased the  $T_M$  by only  $\sim 3^\circ\text{C}$  (Fig. 7 B).

The large increase in stability of the Q263L mutant was accompanied by a marked decrease in its ability to form binary and ternary complexes with the TM N terminus and TnT<sub>70-170</sub>. In the wild-type TM9<sub>a251-284</sub>, formation of the

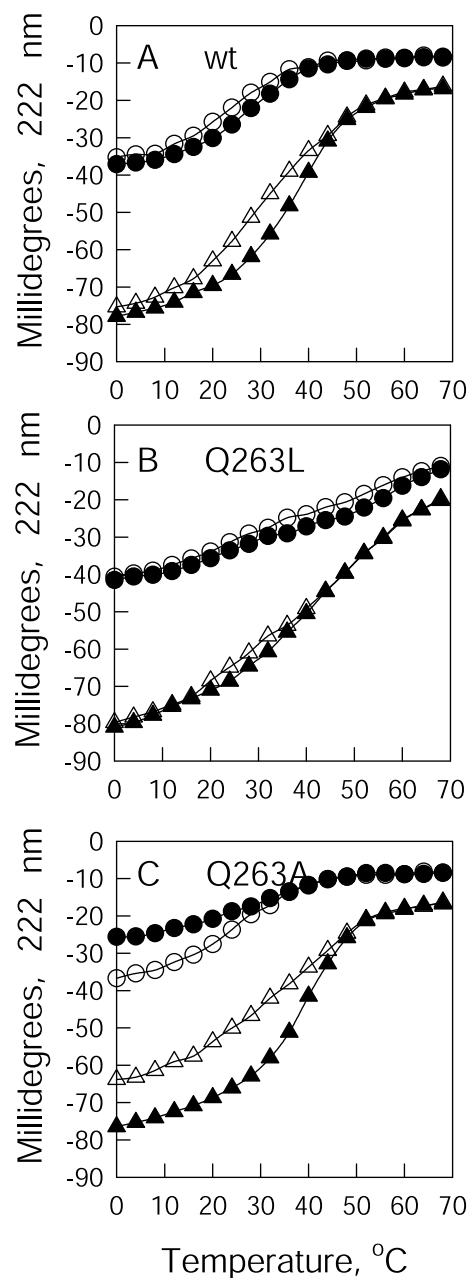


FIGURE 8 The effect of mutations of Q263 on the ellipticity of binary and ternary complexes of TM9<sub>a251-284</sub> with AcTM1<sub>a1-14</sub> and TnT<sub>70-170</sub> at 222 nm as a function of temperature. Replacing glutamine with leucine inhibits the ability of the TM9<sub>a251-284</sub> to form the binary and ternary complexes, but replacing it with alanine has little effect. (A) wild-type TM9<sub>a251-284</sub>; (B) Q263L; (C) Q263A. (○) Sum of the individual unfolding curves of the C- and N-terminal peptides; (●) unfolding of the TM9<sub>a251-284</sub>/TM1<sub>a1-14</sub> overlap complex; (▲) sum of the individual unfolding curves of the TM9<sub>a251-284</sub>/TM1<sub>a1-14</sub> overlap complex and TnT<sub>70-170</sub>; (▲) unfolding of the mixture of the TM9<sub>a251-284</sub>/TM1<sub>a1-14</sub> complex with TnT<sub>70-170</sub>. All of the peptides were 10  $\mu$ M in potassium phosphate buffer, 10 mM, pH 6.5. The results with wild type are similar to those for a related TM9<sub>a251-284</sub> peptide that lacks the initial Gly (Palm et al., 2001).

binary overlap complex with AcTM1<sub>a1-14</sub> caused a small increase ( $\sim 5\%$ ) in ellipticity at 0°C and increased the  $T_M$  of



unfolding of the complex from 23°C to 27°C (comparing the sums of the curves for the individual peptides to the complex) and also increased the cooperativity of unfolding (Fig. 8 A). The changes in stability were used to estimate a dissociation constant for the overlap complex of  $\sim 2 \mu\text{M}$  at 25°C, assuming all the changes in free energy of folding were due to complex formation (Greenfield and Fowler, 2002). Addition of TnT<sub>70-170</sub> to form a ternary complex (Fig. 8 A) increased the  $T_M$  of unfolding of the ternary complex by 6°C from 30°C to 36°C (comparing the sum of the curves for the binary complex and the TnT peptide to the curve for the ternary complex).

In contrast, with the Q263L mutant there were only very small differences between the unfolding curves of the mixtures and the sum of the curves of the unmixed components, indicating poor binary and ternary complex formation (Fig. 8 B.). Surprisingly, when the Q263A mutant was mixed with AcTM1a<sub>1-14</sub> the complex had reproducibly lower ellipticity than the sum of the two unmixed components (although the  $T_M$  was  $\sim 3^\circ\text{C}$  higher), suggesting that the peptides had to partially unfold to bind to each other (Fig. 8 C). The Q263A peptide formed a stable ternary complex with higher helical content and a 5°C higher  $T_M$  of unfolding (38°C vs. 33°C).

#### Nondenaturing gel electrophoresis studies

The effect of the Q263 mutations on complex formation was also directly measured using nondenaturing polyacrylamide gel electrophoresis (Fig. 9). The Tn fragment, TnT<sub>70-170</sub> (10  $\mu\text{M}$ ), was titrated with increasing amounts (5–40  $\mu\text{M}$ ) of the AcTM1a/TM9a complexes, and the components of the mixtures were separated using native gel electrophoresis. Both wild-type and Q263A-TM9a<sub>251-284</sub> formed strong ternary complexes with AcTM1a<sub>1-14</sub> and TnT<sub>70-170</sub>. Most of the TnT fragment was bound when a twofold ratio of either overlap complex was added. In contrast, the Q263L mutant showed no detectable ternary complex until a fourfold ratio of the overlap complex was added, confirming the circular dichroism results. AcTM1a<sub>1-14</sub> is basic and does not enter the gel. The binary and ternary complexes dissociate during electrophoresis and the TM9a<sub>251-284</sub> by itself leaches out of the gel during destaining, so it is not possible to estimate accurate concentrations or dissociation constants from the electrophoresis experiments. Nevertheless, the Q263L mutant clearly shows much lower binding of the TnT peptide than either the wild-type or Q263A peptides.

## DISCUSSION

In this work the secondary structure of the C-terminal 34 residues of striated muscle  $\alpha$ -TM was determined using heteronuclear NMR. The last 15 residues of the C terminus proved to have a very different conformation than the rest of TM, which is coiled coil from residue 1 to 269 (Phillips et al., 1979; Greenfield et al., 1998; Whitby and Phillips,

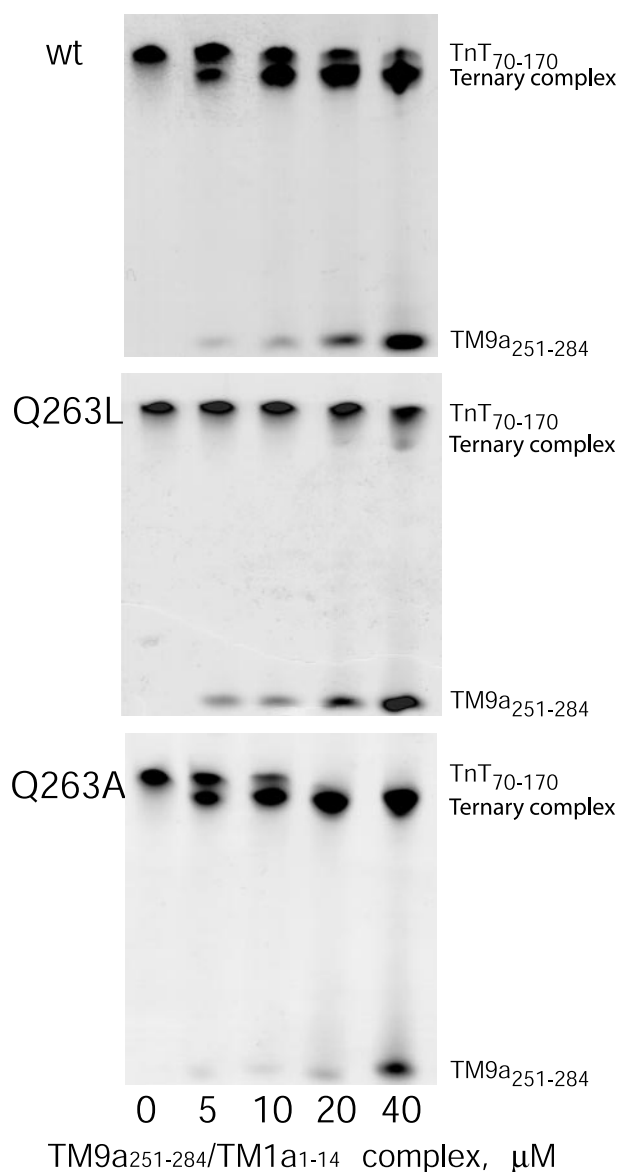


FIGURE 9 Native gel electrophoresis shows that mutating Gln-263 to Leu inhibits the ability of TnT<sub>70-170</sub> to bind a 1:1 mixture of TM9a<sub>251-284</sub> and AcTM1a<sub>1-14</sub> but mutation to Ala has little effect. (Lane 1) TnT<sub>70-170</sub>, 10  $\mu\text{M}$  alone; (lane 2 to 5) TnT<sub>70-170</sub>, 10  $\mu\text{M}$  plus increasing concentrations of TM9a<sub>251-284</sub> plus AcTM1a<sub>1-14</sub> as indicated. The rows containing free TnT<sub>70-170</sub>, free TM9a<sub>251-284</sub>, and the ternary complex are resolved and indicated on the gel. AcTM1a<sub>1-14</sub> is highly basic and runs toward the cathode and is not visible on the gel. The gels contained 10% acrylamide/bis acrylamide (30:0.8), 10% glycerol in Tris-Glycine buffer, pH 8.8. Samples were mixed in potassium phosphate buffer, 10 mM, pH 6.5. Ten microliters were added to each lane. Bands were visualized with Coomassie Brilliant Blue R250.

2000). Residues 270 to 277 appear to be  $\alpha$ -helical, but not part of the coiled-coil domain, whereas the last four residues are not helical and are relatively mobile. The C terminus of TM has long been known to be a major functional determinant of actin affinity and for the isoform-specific interaction of striated muscle TM with Tn (see Introduction). Here we

show that the flexibility of the C terminus is essential for its binding functions.

Whereas isolated TM forms a two-chain coiled coil over most of its length, the C terminus has an unusual sequence that would not be expected to form a stable well-packed two-chain coiled coil. The residues found at the last four C-terminal *a* positions of the heptad repeat are L260, Y267, L288, and M281 and those in the last four *d* positions are Q263, I270, A277, and I284. The glutamine, tyrosine, and alanine residues reduce the stability of model coiled-coil peptides (Tripet et al., 2000; Wagschal et al., 1999). In addition, the last three residues T282, S283, and I284 have low helical propensities and tend to destabilize single-stranded  $\alpha$ -helices (Chou and Fasman, 1974; O'Neil and DeGrado, 1990; Gans et al., 1991). Moreover, the interface residues of the last two heptads have much higher propensities to form three-stranded than two-stranded coiled coils (Tripet et al., 2000; Wagschal et al., 1999). The C-terminal sequence of striated  $\alpha$ -TM, unusual for a two-stranded coiled coil, is required for isoform-specific binding functions (Cho et al., 1990; Cho and Hitchcock-DeGregori, 1991; Hammell and Hitchcock-DeGregori, 1996, 1997; Cho, 2000).

Formation of a complex with the N terminus of  $\alpha$ -TM perturbs the amide backbone resonances of the last 11 residues, consistent with formation of an 11-residue overlap complex, as originally proposed by McLachlan and Stewart (1975). The largest perturbations were seen for M281, T282, S283, and H276. Sano et al. (2000) have shown that modifications of S282 significantly change the end-to-end interactions in TM. However, complex formation does not induce the region to become helical, arguing that in the absence of TnT, the overlap region does not form a four-chain coiled coil. The doubling of several of the backbone amide cross-peaks suggests that the complex is asymmetric. The NMR results are consistent with the model of the overlap region we proposed in Palm et al. (2001) for the ternary complex with TnT with the modification that the strong region of interaction between the N and C termini of TM begins with L274 rather than A277.

Of particular interest are the dramatic changes in the cross-peaks arising from Q263, a residue we postulated would be in a coiled-coil interface region when TnT binds (Palm et al., 2001). The changes in the conformational equilibrium of the glutamine side chains upon complex formation suggested to us that the flexibility of the coiled coil in this region might be essential for complex formation with the N terminus and TnT. Many studies show that protein-protein interactions occur in regions of conformational flexibility (Jurnak, 1994; Betts and Sternberg, 1999; Deprez et al., 2000; Doss-Pepe et al., 2000; Sundberg and Mariuzza, 2000; Camacho and Vajda, 2002), among others. Our findings that the Q263L mutation increased helical stability and reduced complex formation, whereas Q263A is a relatively neutral mutation, show the importance of flex-

ibility (reflected in a certain degree of helical instability) for protein-protein interactions. We have previously reported a similar relationship between helical stability and function in TnT (Palm et al., 2001). Disease-causing mutations in a helical region of TnT<sub>70-170</sub> proposed to form a coiled-coil complex with TM<sub>9a251-284</sub> that increase the stability of the  $\alpha$ -helix reduce the affinity of the TnT peptide for TM.

It has long been known that TM is flexible and that the C-terminal half is more flexible than the N-terminal half (Phillips et al., 1980). The flexibility of TM has long been thought to be important for its ability to regulate contraction (Phillips et al., 1986; for review, see Gergely, 1977; Gordon et al., 2000). Recently, Brown et al. (2001) suggested that clusters of alanine residues in the coiled-coil interface (that would locally destabilize the coiled coil) may allow for multiple discrete bends in the TM molecule contributing to the overall flexibility of TM on the actin filament. The results of our present study show that conformational flexibility of the C terminus of TM is critical for its ability to form a complex with the N terminus of TM and with TnT. In addition to the need for conformational flexibility of the C terminus, we have recently found that other mutations, which decrease the overall conformational flexibility of TM, have drastic effects on its function. For example, replacement of residues 165 to 188 of recombinant rat striated muscle  $\alpha$ -TM with a region of the GCN4 leucine zipper increases its overall  $T_M$  of unfolding by 13° and reduces its actin affinity below a measurable level (unpublished data). Future determination of the atomic resolution structure of the overlap complexes and the conformational dynamics will give insight into the importance of local flexibility for TM binding interactions and cooperative regulatory functions.

We would like to thank Dr. G.T. Montelione at the Center for Advanced Biotechnology and Medicine, Rutgers University, for his continuing collaboration and encouragement and Dr. G.V.T. Swapna for her expert assistance in obtaining the NMR spectra. We would also like to thank Sarah Graboski for expression and purification of the heteronuclearly labeled TM<sub>9a251-284</sub> and TM<sub>1a1-14</sub> peptides. This work was supported by the National Institutes of Health Grant GM 36326 (to S.E.H.D. and N.J.G.) and the shared equipment circular dichroism facility at University of Medicine and Dentistry of New Jersey, which was partially funded by the National Institutes of Health shared equipment award (1 S10 RR16705-01).

## REFERENCES

- Bax, A., G. M. Clore, and A. M. Gronenborn. 1990.  $^1\text{H}$ - $^1\text{H}$  correlation via isotropic mixing of  $^{13}\text{C}$  magnetization, a new three-dimensional approach for assigning  $^1\text{H}$  and  $^{13}\text{C}$  spectra of  $^{13}\text{C}$  enriched proteins. *J. Magn. Reson.* 88:425-431.
- Betts, M. J., and M. J. Sternberg. 1999. An analysis of conformational changes on protein-protein association: implications for predictive docking. *Protein Eng.* 12:271-283.
- Bodenhausen, G., and D. J. Ruben. 1980. Natural abundance nitrogen-15 NMR by enhanced heteronuclear spectroscopy. *Chem. Phys. Lett.* 69: 185-189.

- Böhm, G., R. Muhr, and R. Jaenicke. 1992. Quantitative analysis of protein far UV circular dichroism spectra by neural networks. *Protein Eng.* 5:191–195.
- Boucher, W., E. D. Laue, S. L. Campbell-Burk, and P. J. Dommelle. 1991. Four dimensional heteronuclear triple resonance NMR methods for the assignment of backbone nuclei in proteins. *J. Am. Chem. Soc.* 114: 2262–2264.
- Brown, J. H., K. H. Kim, G. Jun, N. J. Greenfield, R. Dominguez, N. Volkman, S. E. Hitchcock-DeGregori, and C. Cohen. 2001. Deciphering the design of the tropomyosin molecule. *Proc. Natl. Acad. Sci. U. S. A.* 98:8496–8501.
- Camacho, C. J., and S. Vajda. 2002. Protein-protein association kinetics and protein docking. *Curr. Opin. Struct. Biol.* 12:36–40.
- Cho, Y. J. 2000. The carboxyl terminal amino acid residues glutamine276-threonine277 are important for actin affinity of the unacetylated smooth  $\alpha$ -tropomyosin. *J. Biochem. Mol. Biol.* 33:531–536.
- Cho, Y. J., and S. E. Hitchcock-DeGregori. 1991. Relationship between alternatively spliced exons and functional domains in tropomyosin. *Proc. Natl. Acad. Sci. U. S. A.* 88:10153–10157.
- Cho, Y. J., J. Liu, and S. E. Hitchcock-DeGregori. 1990. The amino terminus of muscle tropomyosin is a major determinant for function. *J. Biol. Chem.* 265:538–545.
- Chou, P. Y., and G. D. Fasman. 1974. Conformational parameters for amino acids in helical, beta-sheet, and random coil regions calculated from proteins. *Biochemistry.* 13:211–222.
- Clubb, R. T., V. Thanabal, and G. Wagner. 1992. A constant-time 3D triple-resonance pulse scheme to correlate intrareidue  $^1\text{H}$ ,  $^{15}\text{N}$  and  $^{13}\text{C}$  chemical shifts in  $^{15}\text{N}$ ,  $^{13}\text{C}$ -labeled proteins. *J. Magn. Reson.* 97: 213–217.
- Dabrowska, R., E. Nowak, and W. Drabikowski. 1983. Some functional properties of nonpolymerizable and polymerizable tropomyosin. *J. Muscle Res. Cell. Motil.* 4:143–161.
- de Sousa, A. D., and C. A. Farah. 2001. Tropomyosin containing tryptophan analogs: probes of specific thin filament protein interactions. *Biophys. J.* 82:91a.
- Deprez, P., E. Doss-Pepe, B. Brodsky, and N. C. Inestrosa. 2000. Interaction of the collagen-like tail of asymmetric acetylcholinesterase with heparin depends on triple-helical conformation, sequence and stability. *Biochem. J.* 350:283–290.
- Doss-Pepe, E., P. Deprez, N. C. Inestrosa, and B. Brodsky. 2000. Interaction of collagen-like peptide models of asymmetric acetylcholinesterase with glycosaminoglycans: spectroscopic studies of conformational changes and stability. *Biochemistry.* 39:14884–14892.
- Feng, W., C. B. Rios, and G. T. Montelione. 1996. Phase labeling of C-H and C-C spin-system topologies: application in PFG-HACANH and PFG-HACA(CO)NH triple-resonance experiments for determining backbone resonance assignments in proteins. *J. Biomol. Nucl. Magn. Reson.* 8:98–104.
- Gans, P. J., P. C. Lyu, M. C. Manning, R. W. Woody, and N. R. Kallenbach. 1991. The helix-coil transition in heterogeneous peptides with specific side-chain interactions: theory and comparison with CD spectral data. *Biopolymers.* 31:1605–1614.
- Gergely, J. 1977. Molecular aspects of muscle contraction and regulation. *Basic Res. Cardiol.* 72:109–117.
- Goodman, E. M., and P. S. Kim. 1991. Periodicity of amide proton exchange rates in a coiled-coil leucine zipper peptide. *Biochemistry.* 30:11615–11620.
- Gordon, A. M., E. Homsher, and M. Regnier. 2000. Regulation of contraction in striated muscle. *Physiol. Rev.* 80:853–924.
- Greenfield, N. J., and V. M. Fowler. 2002. Tropomyosin requires an intact N-terminal coiled coil to interact with tropomodulin. *Biophys. J.* 82: 2580–2591.
- Greenfield, N. J., J. H. Huang, T. Palm, G. V. T. Swapna, D. Monleon, G. T. Montelione, and S. E. Hitchcock-DeGregori. 2001. Solution NMR structure and folding dynamics of the N terminus of a rat non-muscle  $\alpha$ -tropomyosin in an engineered chimeric protein. *J. Mol. Biol.* 312: 833–847.
- Greenfield, N. J., G. T. Montelione, R. S. Farid, and S. E. Hitchcock-DeGregori. 1998. The structure of the N-terminus of striated muscle  $\alpha$ -tropomyosin in a chimeric peptide: nuclear magnetic resonance structure and circular dichroism studies. *Biochemistry.* 37:7834–7843.
- Greenfield, N. J., W. F. Stafford, and S. E. Hitchcock-DeGregori. 1994. The effect of N-terminal acetylation on the structure of an N-terminal tropomyosin peptide and  $\alpha$ -tropomyosin. *Protein Sci.* 3:402–410.
- Grzesiek, S., and A. Bax. 1992a. Correlating backbone amide and side-chain resonances in larger proteins by multiple relay triple resonance NMR. *J. Am. Chem. Soc.* 114:6291–6293.
- Grzesiek, S., and A. Bax. 1992b. An efficient experiment for sequential backbone assignment of medium-sized isotopically enriched proteins. *J. Magn. Reson.* 99:201–207.
- Hammell, R. L., and S. E. Hitchcock-DeGregori. 1996. Mapping the functional domains within the carboxyl terminus of  $\alpha$ -tropomyosin encoded by the alternatively spliced ninth exon. *J. Biol. Chem.* 271: 4236–4242.
- Hammell, R. L., and S. E. Hitchcock-DeGregori. 1997. The sequence of the alternatively spliced sixth exon of  $\alpha$ -tropomyosin is critical for cooperative actin binding but not for interaction with troponin. *J. Biol. Chem.* 272:22409–22416.
- Heeley, D. H., L. B. Smillie, and E. M. Lohmeier-Vogel. 1989. Effects of deletion of tropomyosin overlap on regulated actomyosin subfragment 1 ATPase. *Biochem. J.* 258:831–836.
- Hitchcock-DeGregori, S. E. 2002. Tropomyosin. In *Encyclopedia of Molecular Medicine*. T. Creighton, editor. John Wiley and Sons, New York. 3247–3251.
- Hodges, R. S., A. K. Saund, P. C. Chong, S. A. St.-Pierre, and R. E. Reid. 1981. Synthetic model for two-stranded  $\alpha$ -helical coiled-coils. Design, synthesis, and characterization of an 86-residue analog of tropomyosin. *J. Biol. Chem.* 256:1214–1224.
- Holtzer, M. E., D. L. Crimmins, and A. Holtzer. 1995. Structural stability of short subsequences of the tropomyosin chain. *Biopolymers.* 35: 125–136.
- Holtzer, M. E., and A. Holtzer. 1990.  $\alpha$ -helix to random coil transitions of two-chain coiled coils: experiments on the thermal denaturation of isolated segments of  $\alpha$ -tropomyosin. *Biopolymers.* 30: 985–993.
- Ishii, Y., S. Hitchcock-DeGregori, K. Mabuchi, and S. S. Lehrer. 1992. Unfolding domains of recombinant fusion  $\alpha$ -tropomyosin. *Protein Sci.* 1:1319–1325.
- Junius, F. K., S. I. O'Donoghue, M. Nilges, A. S. Weiss, and G. F. King. 1996. High resolution NMR solution structure of the leucine zipper domain of the c-Jun homodimer. *J. Biol. Chem.* 271:13663–13667.
- Jurnak, F. 1994. Protein-protein interaction: complex flexibility. *Nature.* 372:409–410.
- Katayama, E., and S. Nozaki. 1982.  $\text{Ca}^{2+}$ -dependent binding of synthetic peptides corresponding to some regions of troponin-I to troponin-C. *J. Biochem. (Tokyo).* 91:1449–1452.
- Kay, L. E., M. Ikura, and A. Bax. 1990. Proton-proton correlation via carbon-carbon couplings: a three dimensional NMR approach for the assignment of aliphatic resonances in proteins labeled with  $\text{C-}^{13}$ . *J. Am. Chem. Soc.* 112:888–889.
- Kay, L. E., P. Keifer, and T. Saarinen. 1992. Pure absorption gradient enhanced heteronuclear single quantum correlation spectroscopy with improved sensitivity. *J. Am. Chem. Soc.* 114:10663–10665.
- Krishnan, K. S., J. F. Brandts, and S. S. Lehrer. 1978. Effects of an interchain disulfide bond on tropomyosin structure: differential scanning calorimetry. *FEBS Lett.* 91:206–208.
- Landschulz, W. H., P. F. Johnson, and S. L. McKnight. 1988. The leucine zipper: a hypothetical structure common to a new class of DNA binding proteins. *Science.* 240:1759–1764.
- Lehrer, S. S. 1975. Intramolecular crosslinking of tropomyosin via disulfide bond formation: evidence for chain register. *Proc. Natl. Acad. Sci. U. S. A.* 72:3377–3381.



- Lehrer, S. S. 1978. Effects of an interchain disulfide bond on tropomyosin structure: intrinsic fluorescence and circular dichroism studies. *J. Mol. Biol.* 118:209–226.
- Lehrer, S. S., and M. A. Geeves. 1998. The muscle thin filament as a classical cooperative/allosteric regulatory system. *J. Mol. Biol.* 277:1081–1089.
- Lehrer, S. S., N. L. Golitsina, and M. A. Geeves. 1997. Actin-tropomyosin activation of myosin subfragment 1 ATPase and thin filament cooperativity: the role of tropomyosin flexibility and end-to-end interactions. *Biochemistry*. 36:13449–13454.
- Li, Y., S. Mui, J. H. Brown, J. Strand, L. Reshetnikova, L. S. Tobacman, and C. Cohen. 2002. The crystal structure of the C-terminal fragment of striated-muscle  $\alpha$ -tropomyosin reveals a key troponin T recognition site. *Proc. Natl. Acad. Sci. U.S.A.* 99:7378–7383.
- Mak, A. S., and L. B. Smillie. 1981. Non-polymerizable tropomyosin: preparation, some properties and F-actin binding. *Biochem. Biophys. Res. Commun.* 101:208–214.
- Marti, D. N., I. Jelesarov, and H. R. Bosshard. 2000. Interhelical ion pairing in coiled coils: solution structure of a heterodimeric leucine zipper and determination of pK(a) values of glu side chains. *Biochemistry*. 39:12804–12818.
- McLachlan, A. D., and M. Stewart. 1975. Tropomyosin coiled-coil interactions: evidence for an unstaggered structure. *J. Mol. Biol.* 98:293–304.
- Montelione, G. T., and G. Wagner. 1989. Accurate measurements of homonuclear  $^1\text{H}$ - $^1\text{H}$  coupling constants in polypeptides using heteronuclear 2-D NMR experiments. *J. Am. Chem. Soc.* 111:5474–5475.
- Montelione, G. T., and G. Wagner. 1990. Conformation-independent sequential NMR connections in isotope-enriched polypeptides by  $^1\text{H}$ - $^{13}\text{C}$ - $^{15}\text{N}$  triple-resonance experiments. *J. Magn. Reson.* 87:183–188.
- Moraczewska, J., and S. E. Hitchcock-DeGregori. 1998. S1-induced actin binding of tropomyosin depends on its C terminus. *Biophys. J.* 74:532.
- Moraczewska, J., and S. E. Hitchcock-DeGregori. 2000. Independent functions for the N- and C-termini in the overlap region of tropomyosin. *Biochemistry*. 39:6891–6897.
- Moraczewska, J., K. Nicholson-Flynn, and S. E. Hitchcock-DeGregori. 1999. The ends of tropomyosin are major determinants of actin affinity and myosin subfragment 1-induced binding to F-actin in the open state. *Biochemistry*. 38:15885–15892.
- Muhandiram, D. R., and L. E. Kay. 1994. Gradient-enhanced triple-resonance three-dimensional NMR experiments with improved sensitivity. *J. Magn. Reson. Ser. B.* 103:203–216.
- Oas, T. G., L. P. McIntosh, E. K. O'Shea, F. W. Dahlquist, and P. S. Kim. 1990. Secondary structure of a leucine zipper determined by nuclear magnetic resonance spectroscopy. *Biochemistry*. 29:2891–2894.
- Ohyashiki, T., Y. Kanaoka, and T. Sekine. 1976. Studies on calcium ion-induced conformation changes in the actin-tropomyosin-troponin system by fluorimetry: III. Changes in the conformation of tropomyosin associated with functional states. *Biochim. Biophys. Acta.* 420:27–36.
- Oliveira, D. M., C. R. Nakaie, A. D. Sousa, C. S. Farah, and F. C. Reinach. 2000. Mapping the domain of troponin T responsible for the activation of actomyosin ATPase activity: identification of residues involved in binding to actin. *J. Biol. Chem.* 275:27513–27519.
- O'Neil, K. T., and W. F. DeGrado. 1990. A thermodynamic scale for the helix-forming tendencies of the commonly occurring amino acids. *Science*. 250:646–651.
- Palm, T., S. Graboski, S. E. Hitchcock-DeGregori, and N. J. Greenfield. 2001. Disease-causing mutations in cardiac troponin T: identification of a critical tropomyosin-binding region. *Biophys. J.* 81:2827–2837.
- Pan, B. S., A. M. Gordon, and Z. X. Luo. 1989. Removal of tropomyosin overlap modifies cooperative binding of myosin S-1 to reconstituted thin filaments of rabbit striated muscle. *J. Biol. Chem.* 264:8495–8498.
- Perry, S. V. 2001. Vertebrate tropomyosin: distribution, properties and function. *J. Muscle Res. Cell Motil.* 22:5–49.
- Phillips, G. N., Jr. 1986. Construction of an atomic model for tropomyosin and implications for interactions with actin. *J. Mol. Biol.* 192:128–131.
- Phillips, G. N., Jr., and S. Chacko. 1996. Mechanical properties of tropomyosin and implications for muscle regulation. *Biopolymers*. 38:89–95.
- Phillips, G. N., Jr., J. P. Fillers, and C. Cohen. 1980. Motions of tropomyosin: crystal as metaphor. *Biophys. J.* 32:485–502.
- Phillips, G. N., Jr., J. P. Fillers, and C. Cohen. 1986. Tropomyosin crystal structure and muscle regulation. *J. Mol. Biol.* 192:111–131.
- Phillips, G. N., Jr., E. E. Lattman, P. Cummins, K. Y. Lee, and C. Cohen. 1979. Crystal structure and molecular interactions of tropomyosin. *Nature*. 278:413–417.
- Potekhin, S. A., and P. L. Privalov. 1982. Co-operative blocks in tropomyosin. *J. Mol. Biol.* 159:519–535.
- Privalov, P. L. 1982. Stability of proteins: proteins which do not present a single cooperative system. *Adv. Protein Chem.* 35:1–104.
- Rios, C. B., W. Feng, M. Tashiro, Z. Shang, and G. T. Montelione. 1996. Phase labeling of C-H and C-C spin-system topologies: application in constant-time PFG-CBCA(CO)NH experiments for discriminating amino acid spin-system types. *J. Biomol. Nucl. Magn. Reson.* 8:345–350.
- Ruiz-Opazo, N., and B. Nadal-Ginard. 1987.  $\alpha$ -tropomyosin gene organization: alternative splicing of duplicated isotype-specific exons accounts for the production of smooth and striated muscle isoforms. *J. Biol. Chem.* 262:4755–4765.
- Sano, K., K. Maeda, T. Oda, and Y. Maeda. 2000. The effect of single residue substitution of serine-283 on the strength of head-to-tail interaction and actin binding properties of rabbit skeletal muscle  $\alpha$ -tropomyosin. *J. Biochem. (Tokyo)*. 237:1095–1102.
- Schenk, P. M., S. Baumann, R. Mattes, and H. H. Steinbiss. 1995. Improved high-level expression system for eukaryotic genes in *Escherichia coli* using T7 RNA polymerase and rare Arg tRNAs. *Biotechniques*. 19:196–198.
- Schwarzinger, S., G. J. Kroon, T. R. Foss, P. E. Wright, and H. J. Dyson. 2000. Random coil chemical shifts in acidic 8 M urea: implementation of random coil shift data in NMRView. *J. Biomol. Nucl. Magn. Reson.* 18:43–48.
- Stewart, M., and G. C. Roberts. 1983. Nuclear magnetic resonance evidence for a flexible region at the C terminus of  $\alpha$ -tropomyosin. *J. Mol. Biol.* 166:219–225.
- Studier, F. W., A. H. Rosenberg, J. J. Dunn, and J. W. Dubendorff. 1990. Use of T7 RNA polymerase to direct expression of cloned genes. *Methods Enzymol.* 185:60–89.
- Sturtevant, J. M., M. E. Holtzer, and A. Holtzer. 1991. A scanning calorimetric study of the thermally induced unfolding of various forms of tropomyosin. *Biopolymers*. 31:489–495.
- Sundberg, E. J., and R. A. Mariuzza. 2000. Luxury accommodations: the expanding role of structural plasticity in protein-protein interactions. *Struct. Fold Des.* 8:R137–142.
- Tawada, Y., H. Oara, T. Ooi, and K. Tawada. 1975. Non-polymerizable tropomyosin and control of the superprecipitation of actomyosin. *Biochemistry*. 78:65–72.
- Tripet, B., K. Wagschal, P. Lavigne, C. T. Mant, and R. S. Hodges. 2000. Effects of side-chain characteristics on stability and oligomerization state of a de novo-designed model coiled-coil: 20 amino acid substitutions in position "d." *J. Mol. Biol.* 300:377–402.
- Wagschal, K., B. Tripet, P. Lavigne, C. Mant, and R. S. Hodges. 1999. The role of position a in determining the stability and oligomerization state of  $\alpha$ -helical coiled coils: 20 amino acid stability coefficients in the hydrophobic core of proteins. *Protein Sci.* 8:2312–2329.
- Walsh, T. P., C. E. Trueblood, R. Evans, and A. Weber. 1985. Removal of tropomyosin overlap and the co-operative response to increasing calcium concentrations of the acto-subfragment-1 ATPase. *J. Mol. Biol.* 182:265–269.



- Whitby, F. G., and G. N. Phillips, Jr. 2000. Crystal structure of tropomyosin at 7 Angstroms resolution. *Proteins*. 38:49–59.
- Wishart, D. S., and B. D. Sykes. 1994. The  $^{13}\text{C}$  chemical-shift index: a simple method for the identification of protein secondary structure using  $^{13}\text{C}$  chemical-shift data. *J. Biomol. Nucl. Magn. Reson.* 4:171–180.
- Wishart, D. S., B. D. Sykes, and F. M. Richards. 1992. The chemical shift index: a fast and simple method for the assignment of protein secondary structure through NMR spectroscopy. *Biochemistry*. 31:1647–1651.
- Zhou, N. E., C. M. Kay, and R. S. Hodges. 1993. Disulfide bond contribution to protein stability: positional effects of substitution in the hydrophobic core of the two-stranded alpha-helical coiled-coil. *Biochemistry*. 32:3178–3187.
- Zimmerman, D. E., C. A. Kulikowski, Y. Huang, W. Feng, M. Tashiro, S. Shimotakahara, C. Chien, R. Powers, and G. T. Montelione. 1997. Automated analysis of protein NMR assignments using methods from artificial intelligence. *J. Mol. Biol.* 269:592–610.